ACS APPLIED MATERIALS & INTERFACES

RESEARCH ARTICLE

www.acsami.org

Aerogels and Polymorphism of Isotactic Poly(4-methyl-pentene-1)

Christophe Daniel,*,† Jenny G. Vitillo,‡ Gianluca Fasano,† and Gaetano Guerra†

†Dipartimento di Chimica, NANOMATES and INSTM Research Unit, Università di Salerno, Via Ponte Don Melillo, Fisciano (SA) Italy

‡Dipartimento di Chimica IFM and NIS Centre of Excellence, INSTM Research Unit, Università di Torino, Via Giuria 7, Torino 10125, Italy

Supporting Information

ABSTRACT: Monolithic and highly crystalline aerogels of isotactic poly(4-methyl-pentene-1) (i-P4MP1) have been prepared by sudden solvent extraction with supercritical carbon dioxide from thermoreversible gels. The cross-link junctions of i-P4MP1 gels, depending on the solvent, can be constituted by pure polymer crystalline phases (I or III or IV) or by polymer−solvent cocrystalline phases (for cyclohexane and carbon tetrachloride gels). Gels with cocrystalline phases lead to aerogels exhibiting the denser crystalline form II, whereas all the other considered gels lead to aerogels exhibiting the thermodynamically stable form I. Aerogels obtained from form I gels, which do not undergo a crystalline phase transition during the CO_2 extraction process present the high structural stability most suitable for the preparation of porous membranes. The effect of solvents on the aerogel pore structure and morphology has been also investigated by scanning electron microscopy and N_2 sorption measurements. In all cases, the aerogels present highly porous interconnected structures with macropores and mesopores presenting a large size distribution and a vanishing presence of micropores.

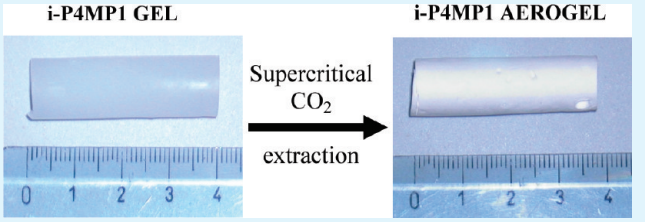

KEYWORDS: monolithic aerogels, membranes, isotactic poly(4-methyl-pentene-1), supercritical CO_2, thermoreversible gels, polymer−solvent cocrystals

INTRODUCTION

Isotactic poly(4-methyl-pentene-1) (i-P4MP1) is a semicrystalline polymer with different properties (high melting point, high clarity, good electrical properties and chemical resistance) being suitable for many applications such as coating of electrical wires, food packaging or optical components.[1] Moreover i-P4MP1 is one of the most permeable plastics to gases and thus is of practical importance as a membrane making polymer.[2,3]

i−P4MP1 presents a complex polymorphic behavior, which is made more complicated by different nomenclatures existing in the literature. Depending on the crystallization procedures, at least four different crystalline forms have been reported. Form I, which is the most stable crystalline form, can be obtained from the melt or from crystallization in high boiling solvents.[4−7] Form I is characterized by polymer chains assuming a 7_2 helical conformation (see Figure 1) and a chain packing in a tetragonal unit cell with a = 18.66 Å and c = 13.80 Å.[4−6] Form II, which can be obtained by isothermal crystallization from dilute xylene solutions at 25 °C, is characterized by a 4_1 helical chain conformation[8−10] and a chain packing in a monoclinic unit cell[9,10] with a = 10.49 Å, b = 18.89 Å and c = 7.13 Å and γ =113.7°.[9] A 4_1 helical chain conformation is also present in form III, which is typically obtained by crystallization from dilute solutions in xylene at 65 °C,[8] in decalin,[11−13] in linear and branched alkanes,[7] as well as in carbon tetrachloride and cycloalkanes.[6] Form III is characterized by a tetragonal unit cell (a = 19.46 Å, c = 7.02 Å).[12,13] Form IV can be obtained either by annealing of form I at high temperature (above 200 °C) under pressure (above 4500 atm)[14] or by crystallization from cyclopentane solutions.[14−16] This crystalline form is characterized by a hexagonal unit cell (a = 22.17 Å, c = 6.5 Å) and a 3_1 chain conformation.[15,16]

As many other polymers, i-P4MP1 can form thermoreversible gels in a large variety of solvents.[15,17−20] Depending on the solvent, the physical cross-links of i-P4MP1 gels can present different crystalline forms.[15,17] For instance, diffraction patterns typical of form I and form IV were obtained after drying of gels with decalin[17] and cyclopentane,[15] respectively. Moreover depending on the gelation conditions, different crystalline structures can be obtained with a same solvent.[19]

It is also worth noting that an additional crystalline structure which have been provisionally indicated as form V have been obtained in cyclohexane gels[17] and by crystallization in cyclohexane and carbon tetrachloride solutions.[21]

The present paper reports on the preparation of i-P4MP1 aerogels, starting from gels obtained with several different solvents with the aim to establish the possible formation of microporous crystalline phases after solvent removal from the gels.

The development of microporous materials with interconnected pores of less than 2 nm size is highly interesting for potential applications in molecular recognition, separation and gas storage. Particularly relevant are the materials based on polymers because of their typical robustness, low cost, and

Received: June 25, 2010
Accepted: March 10, 2011
Published: March 10, 2011

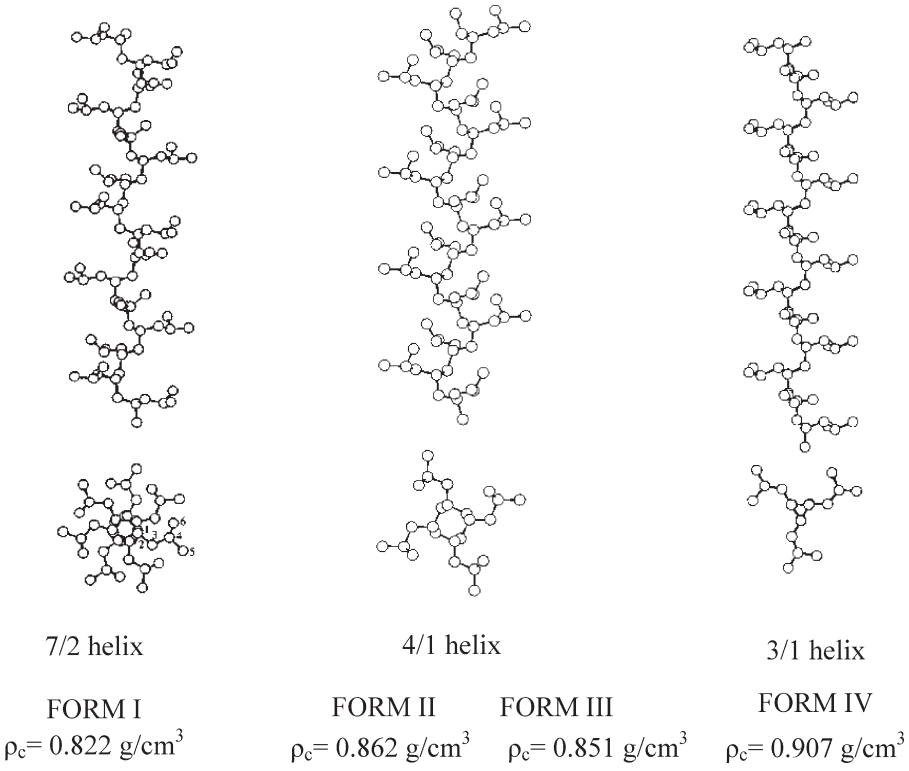

Figure 1. Side view and projection along the chain axis of the chain conformation in the crystalline phases of i-P4MP1. The density ρ_c of the different crystalline forms is also reported.

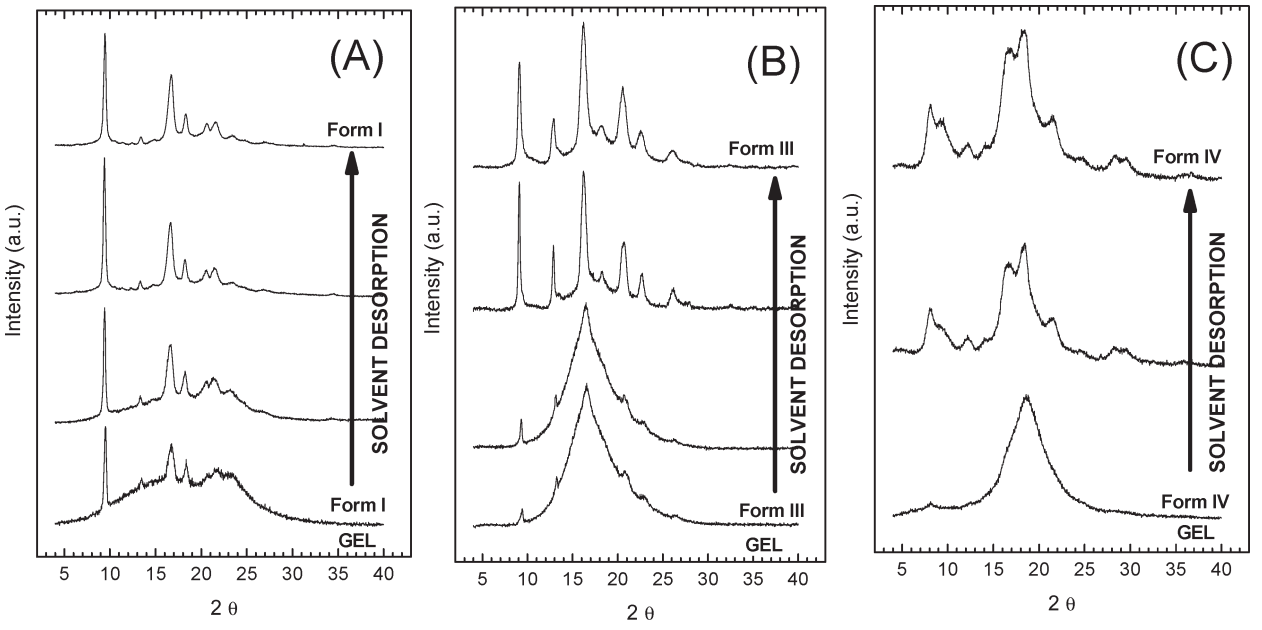

Figure 2. X-ray diffraction patterns of i-P4MP1 gels prepared in (A) 1,3,5-trimethylbenzene, (B) decalin, and (C) cyclopentane, during the progressive desorption of solvent in air.

durability associated with easy processes allowing the preparation of suitable products like films, membranes, foams, and aerogels.

Nanoporous (or microporous according to the IUPAC classification) crystalline polymeric materials based on syndiotactic polystyrene (s-PS) have been recently obtained after suitable guest extraction procedures of the s-PS cocrystalline phases formed with several low-molecular-mass guest molecules.[22,23] These materials rapidly absorb volatile organic molecules, even if present in traces in air or water, and hence are promising for applications in chemical separations[24−27] and molecular sensorics.[28] Moreover the presence of all identical crystalline pores presents,

Table 1. Diffraction Angles ($2\theta_{CuK\alpha}$), Relative Intensities and *hkl* Miller Indexes of the Reflections Observed in the X-ray Diffraction Profiles of Desiccated Gels of Figure 2 and Aerogel Obtained from a Gel with Cyclohexane (CH) (Figure 5, curve d)

desiccated gel with TMB (Figure 2A) form I			aerogel from gel with CH (Figure 5, curve d) form II			desiccated gel with decalin (Figure 2B) form III			desiccated gel with CP (Figure 2C) form IV		
2θ (deg)	I^a	$(hkl)^b$	2θ (deg)	I^a	$(hkl)^c$	2θ (deg)	I^a	$(hkl)^d$	2θ (deg)	I^a	$(hkl)^e$
9.45	vs	200	9.20	vs	100	9.10	vs	200	8.05	s	110
11.50	vw	201	10.30	vs	020	12.90	mw	220, 101	9.40	s	200
12.45	vw	211	10.85	m	$1\bar{2}0$	16.20	vs	211	12.10	mw	210
13.40	w	220	13.20	mw	011	18.30	vw	400,301	16.40	s	310
15.00	w	112,221	14.85	m	$1\bar{1}1$	20.65	mw	420,321	18.20	s	211
16.75	s	212	16.30	ms	$021,1\bar{2}1$	22.70	vw	411	21.15	w	311
20.70	mw	113,411	17.20	w	$111,2\bar{2}0$	26.20	vw	431,112,501	24.50	vw	401
21.65	mw	322,203	18.25	mw	200	32.60	vw	541,710,422	26.85	vw	411
23.50	w		19.70	mw	031	35.00	vw	512,701	28.35	vw	511
25.00	vw	422	20.30	mw	040,121				29.50	vw	202,212
27.00	vw	440	21.20	mw	$2\bar{2}1$				36.40	vw	531,701
34.50	vw		22.70	w	$2\bar{3}1,1\bar{4}1$						
			24.00	vw	041						
			25.80	mw	140						
			29.05	vw	141						

[a] Key: vs = very strong, s = strong, mw = medium weak, w = weak, vw = very weak. [b] *hkl* indices of form I reflections taken from ref 6. [c] *hkl* indices of form II reflections taken from ref 9. [d] *hkl* indices of form III reflections taken from ref 12. [e] *hkl* indices of form IV reflections taken from ref 16.

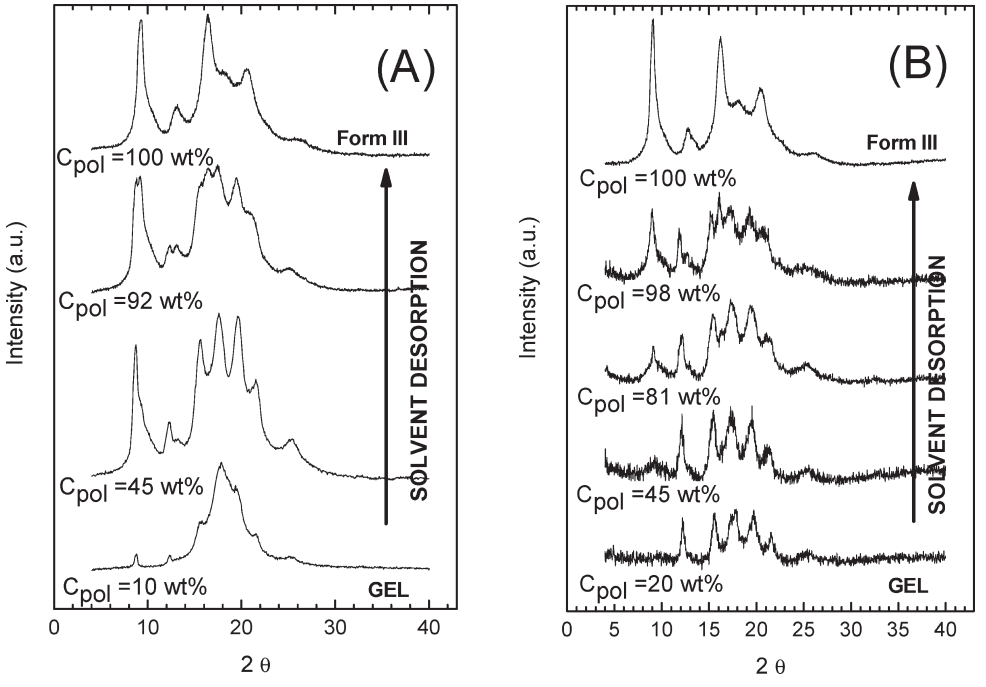

Figure 3. (A) X-ray diffraction patterns of gels prepared in cyclohexane and (B) carbon tetrachloride during progressive solvent desorption in air.

with respect to the materials with microporous polymeric amorphous phases, the advantage of higher guest selectivity.[29−31]

Polymeric microporous materials can be also obtained by supercritical fluid extraction of the solvent included in a gel and, since the first supercritical carbon dioxide drying reported by Pekala,[32,33] many papers have been published on the characterization of organic aerogels prepared in supercritical conditions.[34−36] The main advantage of using supercritical conditions is to avoid the shrinkage of the gels during the solvent removal process. In evaporative drying processes, the tension at the solvent−vapor interface leads to a collapse of the gel network as a result of the disruption of the pore structure of the gel while with supercritical carbon dioxide highly porous materials with large specific area are obtained.

The first examples of polymeric aerogels were based on highly cross-linked polymers (mainly resorcinol-formaldehyde

Table 2. Diffraction Angles ($2\theta_{CuK\alpha}$) and Relative Intensities of the Reflections Observed in the X-ray Diffraction Profiles of Native Gels Obtained with Cyclohexane and Carbon Tetrachloride (Figures 3A and B)

co-crystal with cyclohexane[a]		co-crystal with carbon tetrachloride[b]	
2θ (deg)	I[c]	2θ (deg)	I[c]
8.7	w		
12.35	vw	12.2	s
15.75	vw	15.55	s
17.85	vs	17.45	s
19.4	w	19.7	s
21.50	vw	21.55	mw
25.30	vw	25.5	w

[a] 2θ and I values taken from X-ray diffraction pattern of Figure 3A collected at C_{pol} = 10 wt %. [b] 2θ and I values taken from X-ray diffraction pattern of Figure 3B collected at C_{pol} = 20 wt %. [c] Key: vs = very strong, s = strong, mw = medium weak, w = weak, vw= very weak.

and melamine-formaldehyde aerogels),[32−35] but polymeric aerogels can be also obtained by CO_2 extraction of hydro-[37−42] and organo-[43−51] gels where the gel three-dimensional network is due to electrostatic interactions or to crystalline regions instead of covalent bonds. In particular, in recent years, monolithic aerogels have been obtained with various polysaccharides[38,40,41] and poly(vinylidenefluoride-co-hexafluoropropylene).[46] The large interest in developing polymeric aerogels lies on their various potential applications[36] as porous membranes,[49] catalyst supports,[41] encapsulation medium,[42] or in particle/molecular separation processes.[37]

Recently, it has been also shown that monolithic s-PS aerogels with both amorphous macropores and crystalline micropores can be obtained by supercritical CO_2 extraction of physical gels characterized by cocrystalline phases.[47,50,51] The fast kinetics and high sorption capacity of VOCs from aqueous solutions by s-PS aerogels as well as their good handling characteristics make these new materials particularly suitable as a sorption medium to remove traces of pollutants from water and air.[47,50,51] It is worth adding that, with respect to films or powders, the macropores of s-PS aerogels not only result in an increase in the guest sorption kinetics[47,50,51] (up to several orders of magnitude) but also increase the uptake values for molecules presenting a poor solubility in the polymer amorphous phase.[52]

The first part of the present paper will be focused on the X-ray diffraction investigations of the polymorphism of i−P4MP1 gels prepared with different solvents and of corresponding desiccated gels in order to establish the possible formation of cocrystalline phases. In the second part, highly porous aerogels obtained from the different gels will be prepared by supercritical carbon dioxide and results concerning their crystalline structure, morphology, and porosity will be presented and discussed.

EXPERIMENTAL SECTION

Materials and Sample Preparation. The isotactic poly-(4-methyl-pentene-1) and the solvents used in this study were purchased from Aldrich and used without further purification

All gel samples were prepared in hermetically sealed test tubes by heating the mixtures until complete dissolution of the polymer and appearance of a transparent and homogeneous solution. For cyclopentane gels polymer was dissolved at 85 °C, whereas for the other solvents, polymer was dissolved at 160 °C. Hot polymer solutions were then cooled to room temperature where gelation occurred. For cyclohexane, hot solution was cooled to 95 °C and then cooled to room temperature where gelation occurred.

Aerogel samples were then obtained by treating native gels with a SFX 200 supercritical carbon dioxide extractor (ISCO Inc.) using the following conditions: T = 40 °C, P = 200 bar, extraction time t = 240 min.

For monolithic aerogels with a regular shape (i.e., spherical or cylindrical) the total porosity, including macroporosity, mesoporosity, and microporosity, can be estimated from the volume/mass ratio of the aerogel.

Then, the percentage of porosity P of the aerogel samples can be expressed as[53]

$$P = 100\left(1 - \frac{\rho_{app}}{\rho_{pol}}\right) \quad (1)$$

where ρ_{pol} is the density of the polymer matrix (e.g., equal to 0.83 and 0.85 g/cm^3 for semicrystalline i-P4MP1 samples with a crystallinity of 50%, exhibiting form I and form II phases, respectively) and ρ_{app} is the aerogel apparent density calculated from the mass/volume ratio of the monolithic aerogels.

Techniques. X-ray diffraction patterns were obtained on a Bruker D8 automatic diffractometer operating at a step size of 0.03°and a rate of 164 s/step with a nickel-filtered Cu Kα radiation. Measurements with gels and desiccated gels were done with powder samples while diffraction patterns of aerogels were obtained with 2 mm thick (i.e., thickness of the sample holder) cylinder-shape samples.

The degree of crystallinity of the samples was evaluated from X-ray diffraction data applying the standard procedure of resolving the diffraction pattern into two areas corresponding to the contributions of the crystalline and amorphous fractions.

The correlation length D of the crystalline domains (where an ordered disposition of the atoms is maintained) was evaluated using the Scherrer's equation:

$$D = 0.9\lambda/(\beta\cos\theta) \quad (2)$$

where β is the full width at half-maximum expressed in radian units, λ is the wavelength, and 2θ the diffraction angle. The value of β was corrected from the experimental effects applying the procedure described in ref 54. In particular, a KBr powder sample having a minimum full width at half-maximum, under the same geometrical conditions, of 0.11° was used.

Scanning Electron Microscopy. The internal morphology of the aerogelic monoliths was characterized by means of a scanning electron microscope (SEM, Zeiss Evo50 equipped with an Oxford energy dispersive X-ray detector). Samples were prepared by fracturing small pieces of the monoliths in order to make accessible the internal part of the specimen. Low energy was used (5 keV) in order to obtain the highest possible surface resolution. Before imaging, all the specimens were coated with gold using a VCR high resolution indirect ion-beam sputtering system. The samples were coated depositing approximately 20 nm of gold. The coating procedure was necessary in order to prevent the surface charging during the measurement and to increase the images resolution.

Porosimetry. Surface area, pore volume, and pore size distribution were obtained by N_2 adsorption measurements carried out at 77 K on a Micromeritics ASAP 2020 sorption analyzer. All the samples, in their monolithic form, were outgassed for 24 h at 30 °C before the analysis. In the case of the i-P4MP1/CP monolith a null surface area was obtained for the monolith as-prepared. In this case, the N_2 curves were obtained by fracturing the specimen in order to make accessible the internal pores of the material. The specific surface area of the polymers was calculated using the Brunauer−Emmet−Teller method,[55] while the pore diameter

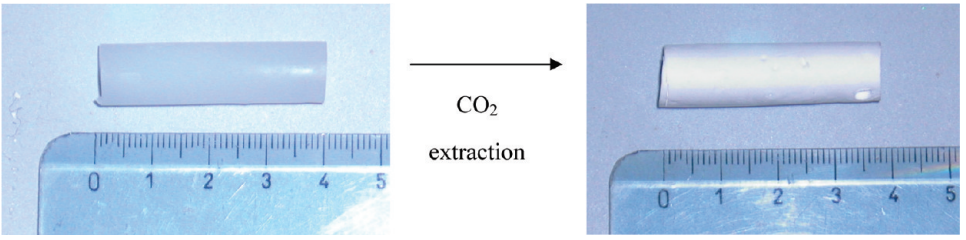

Figure 4. Photographs of a piece of i-P4M1P gel prepared in 1,3,5-trimethylbenzene at C_{pol} = 0.20 g/g, before and after complete solvent extraction via supercritical carbon dioxide (units of the ruler are cm).

and the pore size distribution were evaluated using the DFT (Density Functional Theory) method on the basis of the cylindrical pore model proposed by Jaroniec et al.[56] The micropore volume has been determinate with the t-plot method,[57] adopting a new equation of thickness obtained using as master sample a non porous sPS sample (reported in Table S1 of the Supporting Information). This equation was used in place of the classic Harkins and Jura equation in order to describe more correctly the interactions between the polymer and the nitrogen. The thickness of the single molecular layer has been set to σ = 3.54 Å[58] and t has been obtained as $n/n_m\sigma$ (where n is the number of molecules adsorbed and n_m is the value of n at the monolayer) according to the definition of t.[57]

RESULTS AND DISCUSSION

(A) Gels. *(i) Gels with Pure Polymer Crystalline Phases.* In Figure 2 are reported the X-ray diffraction patterns of i-P4MP1 gels prepared in 1,3,5-trimethylbenzene (TMB) (Figure 2A), decalin (Figure 2B) and cyclopentane (CP) (Figure 2C) during the progressive desorption of solvent at room temperature in air. The Bragg angles, relative intensities, and *hkl* indices of the reflections observed for the totally desiccated gels are listed in Table 1.

We can observe in Figure 2 that the structure of the crystalline junctions formed in i-P4MP1 gels depends on the solvent. Forms I, III, and IV are obtained in native gels prepared with 1,3,5-trimethylbenzene, decalin and cyclopentane, respectively. Then, during progressive solvent desorption the crystalline structures do not undergo any transition and the crystalline forms of the fully dried gels are those initially present in the native gel.

(ii) Gels with polymer–solvent cocrystalline phases. The X-ray diffraction patterns for i-P4MP1/cyclohexane and i-P4MP1/carbon tetrachloride gels during the progressive solvent desorption are reported in Figure 3.

The diffraction patterns of the i-P4MP1 native gels with cyclohexane and carbon tetrachloride display the diffraction peaks listed in Table 2, which become stronger after partial evaporation of the solvent ($C_{pol} \approx$ 45 wt %). When solvent evaporation proceeds (C_{pol} > 90%), new diffraction peaks which can be attributed to form III become visible at 2θ = 9.2, 13.1, and 16.4°.

Finally after complete solvent evaporation (upper curves), only the diffraction peaks typical of form III (see Table 1) are present, whereas all the diffraction peaks initially observed in the native gel have disappeared.

The progressive substitution of the diffraction peaks of both native gels with the peaks of form III, during the progressive solvent desorption, suggests that the native crystalline phases are polymer–solvent cocrystalline phases. This hypothesis is supported by the fact that the positions of the diffraction peaks

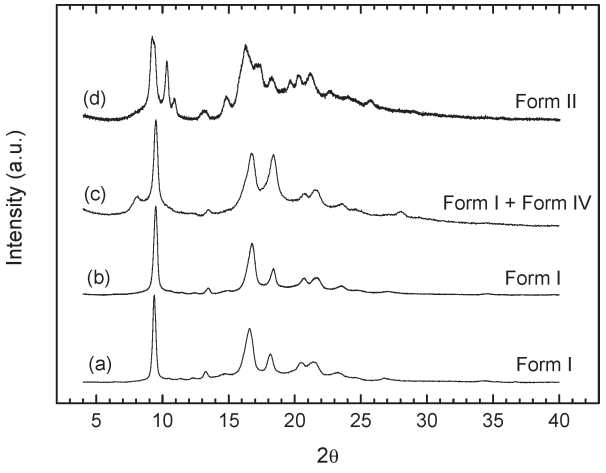

Figure 5. X-ray diffraction patterns of the samples obtained from i-P4MP1 gels prepared in (a) 1,3,5-trimethylbenzene, (b) decalin, (c) cyclopentane, and (d) cyclohexane after complete solvent extraction with supercritical CO_2.

observed in cyclohexane and carbon tetrachloride gels are slightly different (see Table 2).

To further support the hypothesis of formation of two different cocrystalline phases, it is worth noting that the transition into form III is fully reversible. Indeed, exposition of form III desiccated gels to cyclohexane or carbon tetrachloride vapors leads again to the cocrystalline phases, exhibiting the diffraction peaks listed in Table 2.

In this respect, it is worth noting that the crystalline structure of cross-link junctions of cyclohexane and carbon tetrachloride gels have been indicated in literature as form V of i-P4MP1.

(B) Aerogels. Independently on the crystalline structure of the junction zones of the i-P4MP1 gels, complete removal of the solvent was achieved by supercritical CO_2 extraction procedures. The advantage of supercritical CO_2 drying is the absence of surface tension. During the extraction process, a supercritical solution is formed between supercritical CO_2 and liquid solvent and it is thus possible to extract the solvent without collapsing the structure.

As an example, Figure 4 shows that the dimensions of a i-P4MP1 gel prepared in 1,3,5-trimethylbenzene at a polymer concentration C_{pol} = 0.20 g/g remain substantially unchanged during the extraction and a monolithic aerogel with a total porosity of 6.2 cm^3/g and a percentage of porosity of 80% is obtained.

(i) X-ray Diffraction Analysis. The complete extraction of the solvent present in native gels prepared in 1,3,5-trimethylbenzene (starting crystalline form: form I), decalin (starting crystalline

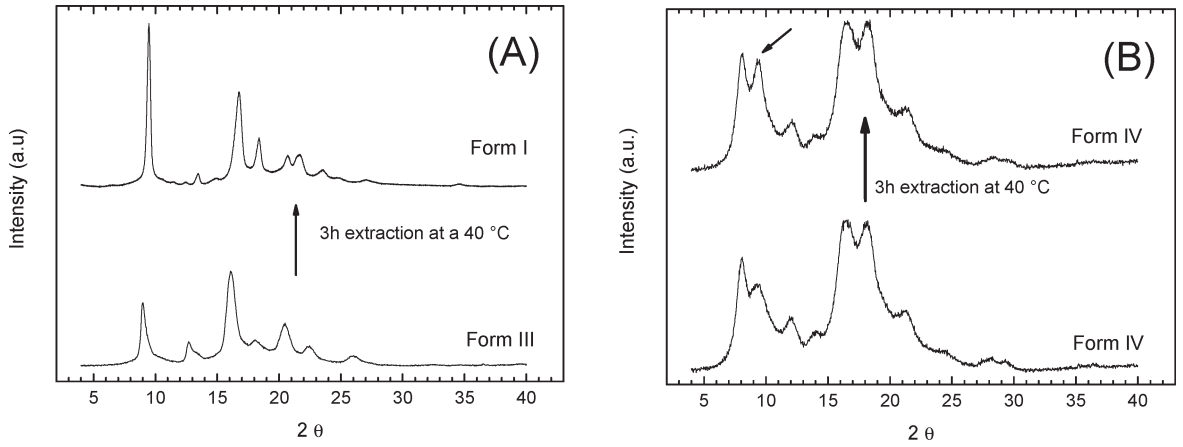

Figure 6. X-ray diffraction patterns of powders exhibiting crystalline forms (A) III and (B) IV, as collected before and after supercritical CO_2 treatment. Form III and form IV powders were obtained by progressive desorption of solvent in air of gels prepared in decalin (leading to form III as shown in Figure 2B) and cyclopentane (leading to form IV as shown in Figure 2C).

Table 3. Crystalline Form, Degree of Crystallinity, Total Porosity ($cm^3\ g^{-1}$, %), Surface Area S_{BET} ($m^2\ g^{-1}$), and Pore Volumes ($cm^3\ g^{-1}$) of i-P4MP1 Aerogels Obtained by Supercritical Carbon Dioxide Treatment of Gels Prepared at C_{pol} = 20 wt % in Different Solvents

	1,3,5-trimethylbenzene	decalin	cyclopentane	cyclohexane
native gel crystalline form	form I	form III	form IV	cocrystal
aerogel crystalline form	form I	form I	form I + form IV	form II
degree of crystallinity (%)	50	50	40	40
correlation length (nm)	31[a]	26[a]	24[a]	32[b]
total porosity[c] (cm^3g^{-1}/ %)	6.2/80	4.9/75	2.8/57	2.4/52
S_{BET}[d] (m^2/g)	87	36	31	36
V_{totN2}[e] ($cm^3\ g^{-1}$)	0.1727	0.0579	0.0745	0.0949
V_{micro}[f] ($cm^3\ g^{-1}$)	0.0026	0.0013	0.0018	0.0019

[a] Correlation length along the direction perpendicular to the form I (200) plane. [b] Correlation length along the direction perpendicular to the form II (020) plane. [c] Total porosity estimated from the volume/mass ratio expressed as cm^3g^{-1} and as % using eq 1. [d] Total area evaluated following the BET model in the standard $0.05 < P/P_0 < 0.25$ pressure range. [e] Pore volume calculated as volume of the N_2 liquid at $p/p_0 \approx 0.98$. [f] Micropore volume obtained from the t-plot.

form: form III), cyclopentane (starting crystalline form: form IV) and cyclohexane (starting crystalline form: cocrystal) has been achieved with supercritical CO_2 at 40 °C and 200 bar for 240 min. X-ray diffraction patterns of the samples after extraction are reported in Figure 5.

We can observe that, unlike progressive solvent desorption (Figure 2), the abrupt extraction with carbon dioxide in supercritical conditions of solvent from gels characterized by pure polymer crystalline phases leads to form I aerogels, independently on the crystalline structure of the native gel although the aerogel from the CP gel also maintains a small amount of the starting form IV crystallites. It is also possible to observe that both the degree of crystallinity and the crystalline domains correlation length of the aerogels are particularly high. Thus, for instance, for the form I aerogel obtained from the gel prepared in 1,3,5-trimethylbenzene (curve a of Figure 5) a crystallinity of c.a. 50% and a correlation length of the crystals perpendicular to the 200 plane (D_{200}) as evaluated using the Scherrer's equation (eq 2) of nearly 31 nm is obtained. Smaller D_{200} values are obtained with the form I aerogels obtained from decalin (D_{200} = 26 nm) and cyclopentane (D_{200} = 24 nm). This could be due to the crystalline transition occurring during solvent extraction.

Unlike i-P4MP1 gels with a pure crystalline phase, when applied to the gels exhibiting cocrystalline phases (with cyclohexane or carbon tetrachloride), the rapid solvent extraction procedure with supercritical carbon dioxide leads to highly crystalline form II aerogels.

This is shown for instance in curve d of Figure 5, where the X-ray diffraction pattern of the sample obtained from a i-P4MP1/cyclohexane gel after solvent extraction by CO_2 at 40 °C and 200 bar, is reported. The diffraction pattern of the aerogel (crystallinity of c.a. 40%) displays well-resolved narrow diffraction peaks indicating the formation of large form II crystals (see Table 1). For instance, the correlation length of the crystals perpendicular to the 020 plane, as evaluated on the basis of the half-height width of the 020 peak (at $2\theta_{CuK\alpha}$ = 10.3°), is c. a. 32 nm.

It is worth noting that differential scanning calorimetry (see Figure S1 in the Supporting Information) and X-ray diffraction analysis (see Figure S2 in the Supporting Information) have shown that the II → I transition temperature for form II aerogels occurs at 143 °C which is definitely higher than those observed for form II samples obtained in different conditions (in the range 120−125 °C).[8,59]

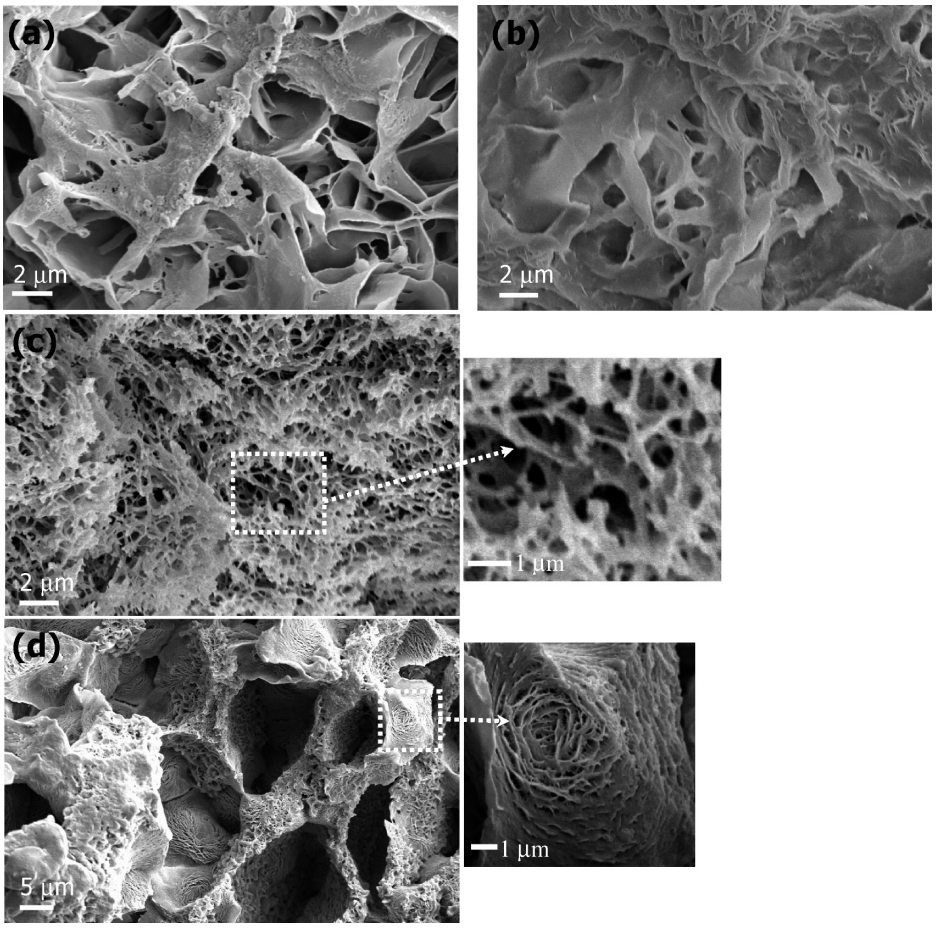

Figure 7. SEM micrographs of aerogels obtained from gels prepared in (a) 1,3,5-trimethylbenzene, (b) decalin, (c) cyclopentane, and (d) cyclohexane at C_{pol} = 20 wt %. Magnification of aerogels obtained from cyclopentane and cyclohexane gels are also reported.

It has been reported in a previous work that different i-P4MP1 recrystallization phenomena may occur depending on the CO_2 pressure and on the relative contents of solvent and CO_2.[20]

The transition to form I observed here for the form III gel during CO_2 extraction is not surprising. In fact, the same treatment with supercritical CO_2, when conducted on powders exhibiting form III (e.g., the fully desiccated decalin gel of Figure 2B) leads to the thermodynamically stable form I (Figure 6A). This can be easily rationalized by the plasticization of the amorphous phase induced by CO_2, which decreases the glass-transition temperature ($T_g \approx 50-70$ °C) and hence destabilizes form III, which is only kinetically stable.

The supercritical CO_2 treatment on form IV powders (e.g., the fully desiccated cyclopentane gel of Figure 2C) leaves substantially unaltered the diffraction pattern (Figure 6B) although we can observe a small increase and a sharpening of the diffraction peak located at $2\theta = 9.4°$ (indicated with an arrow), which could correspond to an increase of the form IV crystals along the direction perpendicular to the 200 plane or to the formation of traces of form I. The complete IV → I transition observed in cyclopentane gels (curve c of Figure 5), could be due to a combined effect of the CO_2-induced plasticization and abrupt solvent removal.

(ii) Porosity and Morphology Characterization. As shown in Figure 4, monolithic aerogels can be obtained after solvent extraction with supercritical CO_2. However, depending on the solvent, volume shrinkage may occur during extraction leading to a variation of the aerogel total porosity as shown in row 5 of Table 3. It is worth noting that volume shrinkage occurs only with the samples which undergo a crystalline phase transition.

The scanning electron micrographs (SEM) are reported in Figure 7 for the different aerogels obtained after CO_2 extraction of gels prepared at C_{pol} = 20 wt % in 1,3,5-trimethylbenzene (Figure 7a), decalin (Figure 7b), cyclopentane (Figure 7c), and cyclohexane (Figure 7d).

For aerogels obtained from i-P4MP1/1,3,5-trimethylbenzene and i-P4MP1/decalin gels we can observe a lamellar structure with macropores of about 0.5−4 μm. For the aerogel obtained from cyclopentane an open network of fibrils with diameter of c. a. 100 nm with a large number of fiber bundles is observed. Most pores of the network are 0.2−0.5 μm wide.

In the end, for cyclohexane aerogels, large honeycomb-type pores with size 8−12 μm are clearly observed while on magnification of the walls smaller macropores with dimensions 0.1 to 0.2 μm can be observed between the lamellae.

Sorption−desorption N_2 isotherms (where the sorption is expressed as cm^3 of nitrogen in normal conditions per gram of polymer) are reported in Figure 8A, whereas the corresponding values for the surface area, total pore volume, and micropore volume are reported in Table 3. The pore size distributions obtained by applying the NLDFT method are reported in Figure 8B.

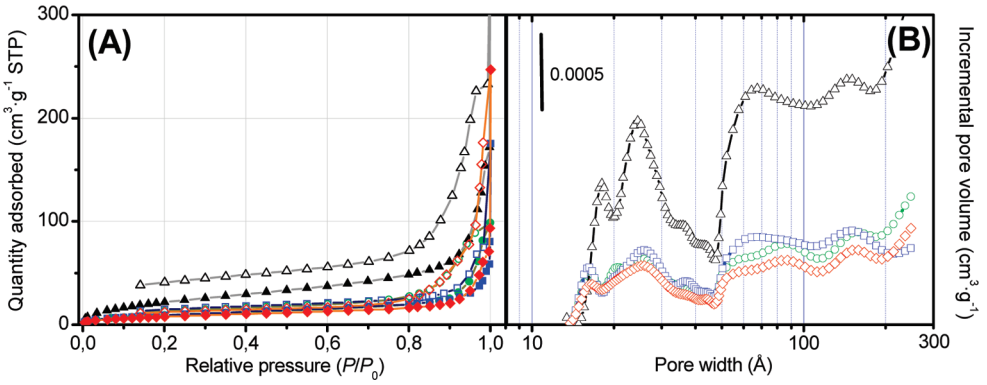

Figure 8. (A) Volumetric N_2 adsorption isotherms recorded at 77 K of the aerogels obtained from 20 wt % gels prepared with cyclohexane (circles, green), 1,3,5-trimethylbenzene (triangles, black), decalin (squares, blue) and cyclopentane (diamonds, red). Filled and empty scatters refer to the adsorption and desorption branches, respectively. (B). Pore size distributions obtained by applying the NLDFT method (non-local density functional theory, cylindrical pore model, pillared clay surface)[60] to the isotherms reported in part A.

It is worth noting that N_2 physisorption at 77 K allows to characterize only pores in the mesopore and micropore range. SEM measurements (Figure 7) have clearly shown the large amount of macropores in these materials: accordingly the pore volumes (V_{totN2}) calculated as volume of the liquid N_2 at $p/p_0 \approx 0.98$ (row 7 of Table 3) differ greatly from the total porosity of the aerogels (row 5 of Table 3). The difference between the total porosity and the V_{totN2} values reported in Table 3 then represents an estimate of the macropore volume. In particular, the porosity data of Table 3 show that mesoporosity represents only a small fraction of the total porosity (i.e., less than 3%). This agrees with the SEM micrographs of Figure 7 that show the strong macroporous nature of all the specimens.

The shape of the isotherms (type IV and with a large hysteresis loop) indicates the prevalent mesoporous nature of all the specimens and the almost vanishing presence of microporosity. This was confirmed by both the t-plot and the DFT analyses: in fact, if on one hand the t-plot indicates the microporous volume to be less than the 3% of the total pore volume, the distribution of the pores obtained by the DFT method results to be qualitatively very similar for all the aerogels and characterized by a broad and uniform family of pores covering the whole mesopore range (>20 Å). A small component due to the micropores is present in the range 16−20 Å but is only minoritary. For the i-P4MP1/1,3,5-trimethylbenzene aerogel the persistence of the hysteresis at low p/p_0 values is an indication of the hindered diffusivity of nitrogen due to the monolithic nature of the specimen.

CONCLUSIONS

Monolithic aerogels of i-P4MP1 have been obtained by solvent extraction with supercritical carbon dioxide from gels. These aerogels can combine high degrees of porosity with high degrees of crystallinity and exhibit crystalline phases whose nature is determined by the nature of the crystalline cross-link junctions of the native gels.

In particular, if the cross-linking crystalline phases are constituted by a pure polymer form (I, III, or IV), all the gels present similar polymorphic behavior, as a consequence of solvent removal. In fact, all their native crystalline phases are maintained after slow room temperature desiccation while they are all transformed into the thermodynamically stable form I, after abrupt solvent removal by supercritical carbon dioxide. On the contrary, if the cross-linking crystalline phases are constituted by host−guest cocrystalline forms (with cyclohexane or carbon tetrachloride), the gels also present similar polymorphic behavior as a consequence of solvent removal. However, in this case, the native cocrystalline phases are transformed into form III after slow room temperature desiccation, whereas they are transformed into form II after abrupt solvent removal by supercritical carbon dioxide.

Scanning electron microscopy has clearly established the macroporosity of the aerogel with large differences in pore size distribution. Thus for the aerogel obtained from i-P4MP1/cyclohexane gels, macropores with dimensions larger than 10 μm were observed, whereas for aerogels obtained from i-P4MP1/cyclopentane gels, most macropores are 0.2−0.5 μm wide.

N_2 porosity measurements have highlighted only a vanishing presence of micropores, and more particularly the absence of nanoholes arising from solvent extraction from the cocrystalline phase of the gel obtained from cyclohexane while for all the areogels the presence of mesopores with large size heterogeneity have been established.

Finally, it is worth noting that important volume shrinkage have been observed with aerogels obtained from gels which undergo a crystalline phase transition during the extraction process, specially i-P4MP1/cyclopentane and i-P4MP1/cyclohexane gels, whereas only form I gels like those obtained in 1,3,5-trimethylbenzene maintain both the dimension and shape of the native gel. Thus, only form I gels present a high structural stability necessary to prepare porous i-P4MP1 membranes.

ASSOCIATED CONTENT

Supporting Information. Universal thickness curve adopted for the t-plot analysis, DSC thermogram of form II aerogel, and X-ray diffraction pattern after annealing of form II aerogel (PDF). This material is available free of charge via the Internet at http://pubs.acs.org.

AUTHOR INFORMATION

Corresponding Author
*E-mail: cdaniel@unisa.it.

■ ACKNOWLEDGMENT

Financial support of the "Ministero dell'Istruzione, dell'Università e della Ricerca" (PRIN2007) is gratefully acknowledged. We thank Prof. Vincenzo Venditto of University of Salerno for useful discussions. Dr. Federico Cesano of University of Torino is acknowledged for the help in SEM measurements.

■ REFERENCES

(1) Lopez, L. C.; Wilkes, G. L.; Stricklen, P. M.; White, S. C. *J. Macromol. Sci.—Rev. Macromol. Chem. Phys.* **1992**, *C32*, 301–406.
(2) Skiens, W. E.; Lipps, B. J.; Clark, M. E.; McLain, E. A. *J. Biomed. Mater. Res. Symp.* **1971**, *1*, 135–148.
(3) Puleo, P. K.; Paul, D. R.; Wong, P. K. *Polymer* **1989**, *30*, 1357–1366.
(4) Natta, G.; Corradini, P.; Bassi, W. *Rend. Fis. Accad. Lincei* **1955**, *19*, 404–411.
(5) Bassi, W.; Bonsignori, O.; Lorenzi, G. P.; Pino, P.; Corradini, P.; Temussi, P. A. *J. Polym. Sci., Polym. Phys. Ed.* **1971**, *9*, 193–208.
(6) Kusanagi, H.; Takase, M.; Chatani, Y.; Tadokoro, H. *J. Polym. Sci. Polym. Phys. Ed.* **1978**, *16*, 131–146.
(7) Charlet, G.; Delmas, G.; Revol, F. J.; Manley, R., St. *J. Polymer* **1984**, *25*, 1613–1618.
(8) Takayanagi, M.; Kawasaki, N. *J. Macromol. Sci. Phys.* **1967**, *B1*, 741–758.
(9) De Rosa, C. *Macromolecules* **2003**, *36*, 6087–6094.
(10) Ruan, J.; Thierry, A.; Lotz, B. *Polymer* **2006**, *47*, 5478–5493.
(11) Nakajima, A.; Hayashi, S.; Taka, T.; Utsumi, N. *Kolloid Z. Z. Polym.* **1969**, *234*, 1097–1108.
(12) De Rosa, C.; Borriello, A.; Venditto, V.; Corradini, P. *Macromolecules* **1994**, *27*, 3864–3868.
(13) De Rosa, C.; Auriemma, F.; Borriello, A.; Corradini, P. *Polymer* **1995**, *36*, 4723–4727.
(14) Hasegawa, R.; Tanabe, Y.; Kobayashi, M.; Tadokoro, M.; Sawaoka, A.; Kawai, N. *J. Polym. Sci., Polym. Phys. Ed.* **1970**, *8*, 1073–1087.
(15) Charlet, G.; Delmas, G. *Polym. Bull. (Berlin)* **1982**, *6*, 367–373.
(16) De Rosa, C. *Macromolecules* **1999**, *32*, 935–938.
(17) Aharoni, S. M.; Charlet, G.; Delmas, G. *Macromolecules* **1981**, *14*, 1390–1394.
(18) Charlet, G.; Phuong-Nguyen, H.; Delmas, G. *Macromolecules* **1984**, *17*, 1200–1208.
(19) Tanigami, T.; Suzuki, H.; Yamaura, K.; Matsuzawa, S. *Macromolecules* **1985**, *18*, 2595–2600.
(20) Fang, J.; Kiran, E. *J. Supercrit. Fluids* **2006**, *38*, 132–135.
(21) Charlet, G.; Delmas, G. *Polymer* **1984**, *25*, 1619–1625.
(22) De Rosa, C.; Guerra, G.; Petraccone, V.; Pirozzi, B. *Macromolecules* **1997**, *30*, 4147–4152.
(23) Petraccone, V.; Ruiz de Ballesteros, O.; Tarallo, O.; Rizzo, P.; Guerra, G. *Chem. Mater.* **2008**, *20*, 3663–3668.
(24) Manfredi, C.; Del Nobile, M. A.; Mensitieri, G.; Guerra, G.; Rapacciuolo, M. *J. Polym. Sci. Polym. Phys. Ed.* **1997**, *35*, 133–140.
(25) Sivakumar, M.; Yamamoto, Y.; Amutharani, D.; Tsujita, Y.; Yoshimizu, H.; Kinoshita, T. *Macromol. Rapid Commun.* **2002**, *23*, 77–79.
(26) Uda, Y.; Kaneko, F.; Kawaguchi, T. *Macromol. Rapid Commun.* **2004**, *25*, 1900–1904.
(27) Borriello, A.; Agoretti, P.; Ambrosio, L.; Fasano, G.; Pellegrino, P.; Venditto, V.; Guerra, G. *Chem. Mater.* **2009**, *21*, 3191–3196.
(28) Pilla, P.; Cusano, A.; Cutolo, A.; Giordano, M.; Mensitieri, G.; Rizzo, P.; Sanguigno, L.; Venditto, V.; Guerra, G. *Sensors* **2009**, *9*, 9816–9857.
(29) Guerra, G.; Milano, G.; Venditto, V.; Musto, P.; De Rosa, C.; Cavallo, L. *Chem. Mater.* **2000**, *12*, 363–368.
(30) Mahesh, K. P. O.; Sivakumar, M.; Yamamoto, Y.; Tsujita, Y.; Yoshimizu, H.; Okamoto, S. *J. Membr .Sci.* **2005**, *262*, 11–19.
(31) Rizzo, P.; Daniel, C.; De Girolamo Del Mauro, A; Guerra, G. *Chem. Mater.* **2007**, *19*, 3864–3866.
(32) Pekala, R. W. U.S. patent 4 873 218, 1989.
(33) Pekala, R. W. *J. Mater. Sci.* **1989**, *24*, 3221–3227.
(34) R.W. Pekala, R. W.; Alviso, C. T.; Kong, F. M.; Hulsey, S. S. *J. Non-Cryst. Solids* **1992**, *145*, 90–98.
(35) Pekala, R. W.; Schaefer, D. W. *Macromolecules* **1993**, *26*, 5487–5493.
(36) Pierre, A. C.; Pajonk, G. M. *Chem. Rev.* **2002**, *102*, 4243–4265.
(37) Jin, H.; Nishiyama, Y.; Wada, M.; Kuga, S. *Colloids Surf., A* **2004**, *240*, 63–67.
(38) Gavillon, R.; Budtova, T. *Biomacromolecules* **2008**, *9*, 269–277.
(39) Miao, Z. J.; Ding, K. L.; Wu, T. B.; Liu, Z. M.; Han, B. X.; An, G. M.; Miao, S. D.; Yang, G. Y. *Microporous Mesoporous Mater.* **2008**, *111*, 104–109.
(40) Robitzer, M.; David, L; Rochas, C.; Di Renzo, F.; Quignard, F. *Langmuir* **2008**, *24*, 12547–12552.
(41) Quignard, F.; Valentin, R.; Di Renzo, F. *New J. Chem.* **2008**, *32*, 1300–1310.
(42) Paakko, M.; Vapaavuori, J.; Silvennoinen, R.; Kosonen, H.; Ankerfors, M.; Lindstrom, T.; Berglund, L. A.; Ikkala, O. *Soft Matter* **2008**, *4* (12), 2492–2499.
(43) Beaucage, G.; Aubert, J. H.; Lacasse, R. R.; Schaefer, D. W.; Rieker, T. P.; Erlich, P.; Stein, R. S.; Kulkarni, S.; Whaley, P. D. *J. Polym. Sci., Part B: Polym. Phys.* **1996**, *34*, 3063–3072.
(44) Dasgupta, D; Nandi, A. K. *Macromolecules* **2005**, *36*, 6504–6512.
(45) Dasgupta, D; Nandi, A. K. *Macromolecules* **2007**, *40*, 2008–2018.
(46) Cardea, S.; Gugliuzza, A.; Sessa, M.; Aceto, M. C.; Drioli, E.; Reverchon, E. *ACS Appl. Mater. Interfaces* **2009**, *1*, 171–180.
(47) Daniel, C.; Alfano, D.; Venditto, V.; Cardea, S.; Reverchon, E.; Larobina, D.; Mensitieri, G.; Guerra, G. *Adv. Mater.* **2005**, *17*, 1515–1518.
(48) Malik, S.; Rochas, C.; Guenet, J.-M. *Macromolecules* **2005**, *38*, 4888–4893.
(49) Malik, S.; Roizard, D.; Guenet, J.-M. *Macromolecules* **2006**, *39*, 5957–5959.
(50) Daniel, C.; Sannino, D.; Guerra, G. *Chem. Mater.* **2008**, *20*, 577–582.
(51) Daniel, C.; Giudice, S.; Guerra, G. *Chem. Mater.* **2009**, *21*, 1028–1034.
(52) Figueroa-Gerstenmaier, S.; Daniel, C.; Milano, G.; Vitillo, J. G.; Zavorotynska, O.; Spoto, G.; Guerra, G. *Macromolecules* **2010**, *43*, 8594–8601.
(53) Ko, E. I. In *Kirk-Othmer Encyclopedia of Chemical Technology*, 4th ed.; John Wiley & Sons: New York, 1998; Suppl. Vol., "Aerogels", pp 1–22.
(54) Klug, H. P.; Alexander, L. E. In *X-ray Diffraction Procedure*; John Wiley: New York, 1959; Chapter 9.
(55) Brunauer, S.; Emmett, P. H.; Teller, E. *J. Am. Chem. Soc.* **1938**, *60*, 309–319.
(56) Jaroniec, M.; Kruk, M.; Olivier, J. P.; Koch, S. In *Fifth InternationalSymposium on the Characterization of Porous Solids, COPS-V*; Heidelburg, Germany, 2009; Studies in Surface Science and Catalysis; Elsevier: Amsterdam, 2000; p 71.
(57) Gregg, S. J.; Sing, K. S. W. In *Adsorption, Surface Area and Porosity*: Academic Press: London, 1982; p 113.
(58) Lippens, B. C.; De Boer, J. H. *J. Catal.* **1965**, *4*, 319–323.
(59) Miller, R. L. In *Polymer Handbook*, 3rd ed.; John Wiley: New York, 1989; Vol. VI, p 1.
(60) Olivier, J. P.; Occelli, M. L. *J. Phys. Chem. B* **2001**, *105*, 623–629.